Qualifying composition dependent p and n self-doping in CH3NH3PbI3

Qi Wang, Yuchuan Shao, Haipeng Xie, Lu Lyu, Xiaoliang Liu, Yongli Gao, and Jinsong Huang

Articles you may be interested in

Qualifying composition dependent *p* and *n* self-doping in CH₃NH₃PbI₃

Qi Wang,[1] Yuchuan Shao,[1] Haipeng Xie,[2] Lu Lyu,[2] Xiaoliang Liu,[2] Yongli Gao,[3] and Jinsong Huang[1,a)]

[1]*Department of Mechanical and Materials Engineering and Nebraska Center for Materials and Nanoscience, University of Nebraska-Lincoln, Lincoln, Nebraska 68588-0656, USA*
[2]*Hunan Key Laboratory for Super-microstructure and Ultrafast Process, College of Physics and Electronics, Central South University, Changsha 410083, People's Republic of China*
[3]*Department of Physics and Astronomy, University of Rochester, Rochester, New York 14627, USA*

We report the observation of self-doping in perovskite. CH₃NH₃PbI₃ was found to be either *n*- or *p*-doped by changing the ratio of methylammonium halide (MAI) and lead iodine (PbI₂) which are the two precursors for perovskite formation. MAI-rich and PbI₂-rich perovskite films are p and n self-doped, respectively. Thermal annealing can convert the *p*-type perovskite to *n*-type by removing MAI. The carrier concentration varied as much as six orders of magnitude. A clear correlation between doping level and device performance was also observed. © *2014 AIP Publishing LLC.*
[http://dx.doi.org/10.1063/1.4899051]

The development of photovoltaic (PV) technology has drawn considerable attention in the past decades because of its potential in harnessing solar energy to solve today's energy crisis. Historically, breakthrough of the silicon PV technology occurred in the very moment that the doping was no longer determined by unintentional impurities.[1] Nowadays, intentional doping techniques have been widely used in both inorganic and organic semiconductor based PV devices.[1–6] Doping in semiconductors directly change many electronic properties, such as charge recombination rate,[2] carrier diffusion length,[3] open circuit voltage (V_{OC}),[4,5] interface energy barrier, and contact resistance.[6] Therefore, understanding the doping mechanism of a semiconductor is crucial in predicting its electronic properties for rational design of efficient PV devices. Recently, methylammonium lead halides (CH₃NH₃PbI₃, or MAPbI₃) have arisen as one of the most attractive candidates for the next generation low-cost solution process PV materials. Devices applying these perovskite materials have achieved a remarkably high power conversion efficiency of 15%–18% in both mesoporous structure and planar heterojunction structure.[7–11] In attempt to find out why the solution processed polycrystalline CH₃NH₃PbI₃ works so well as a PV material, theoretical calculations by Hong *et al.* and Yin *et al.* revealed that this unique family of material is tolerant to defects because the intrinsic point defects do not generate gap states.[12–14] One very interesting result from these theoretical calculations is that bulk perovskite can be self-doped by defects engineering. It was predicted that the electronic conductivity of perovskite can be tuned between *p*-type and *n*-type by controlling growth conditions, but no clue was provided on how the material growth condition impacts the doping of perovskite, nor the impact of doping on device performance was predicted or studied.

In this manuscript, we gave the experimental evidence that CH₃NH₃PbI₃ can be either *n*- or *p*-self-doped by changing the ratio of two precursors for perovskite formation. The

electronic properties of perovskite films were found to be tuned by the film composition that was strongly influenced by the film formation methods, precursor composition, and process conditions.

One unique property of MAPbI₃ is that its formation involves reaction of an organic and an inorganic precursor, i.e., methylammonium halide (MAI) and lead iodine (PbI₂). Therefore, the composition and material defects of solution deposited perovskite could be largely tuned by changing the PbI₂/MAI precursor ratio in the precursor mixture solution. MAPbI₃ films in this study were formed by two low-temperature solution approaches: the single-step pre-mixed precursor deposition and the two-step interdiffusion deposition. Details about material synthesis and perovskite film fabrication could be found elsewhere.[15–17] In short, in the pre-mixed precursor deposition method, MAI and PbI₂ precursors were dissolved in anhydrous *N,N*-dimethylformamide (DMF), and mixed in different PbI₂/ MAI ratios from 0.3 to 1.7. Our previous X-ray diffraction (XRD) study of perovskite films made by different precursor ratios indicated that there is an obvious transition to phase pure perovskite when precursor ratio increased to 0.52.[15] Therefore, it is expected that the precursor ratio that leads to a stoichiometry perovskite film is above 0.52. For interdiffusion deposition, PbI₂ and MAI were dissolved in orthogonal solvents of DMF and 2-propanol. The precursors were then sequentially spun onto the substrates with the PbI₂ layer underneath the MAI layer, followed by a thermal annealing driven diffusion process. The charge carrier concentration and mobility of the perovskite films were studied by the Hall effect measurement, which was performed with six contacts Hall bar method. Figure 1(a) illustrates the setup used in this study and shows a typical measurement result. A 100 nm thick gold layer was thermally evaporated onto the perovskite films to serve as metal contacts. The distances between contacts 1 and 4, contacts 3 and 5, and contacts 2 and 3 were 1 mm, 0.3 mm, and 0.45 mm, respectively. It is worthy to mention that our setup possesses a rotating magnet design, which could subtract the Hall voltage base line caused by nonsymmetrical sample

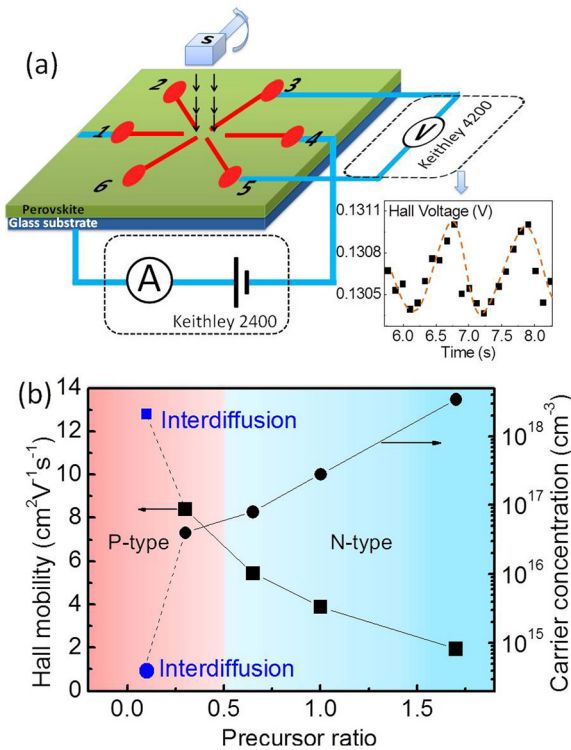a)Author to whom correspondence should be addressed. Electronic mail: jhuang2@unl.edu

FIG. 1. (a) Schematic Hall effect measurement setup and a typical Hall voltage test result. (b) Composition dependent carrier concentration (circle) and carrier mobility (square) in perovskite films formed by one-step pre-mixed precursor deposition (black) and two-steps interdiffusion method (blue).

geometry, and greatly reduce the Hall voltage noise. Carrier concentration and mobility in the Hall effect measurement can be calculated from the equations

$$n = \frac{rIB}{DqV_H}, \tag{1}$$

$$\mu = \frac{1}{\rho q n}, \tag{2}$$

where n is majority carrier concentration, r is Hall scattering factor which is assumed to be 1 here as this number typically lies between 1 and 2, I is DC current, B is magnetic field, D is thickness of films, q is electron charge, V_H is the Hall voltage measured between contacts 2 and 6 in Figure 1, μ is mobility, and ρ is resistivity which was tested by four probe method.

We first studied the doping effect in perovskite films formed by the single-step deposition method with premixed precursor solution at different precursor ratios. Figure 1(b) shows the mobility and carrier concentration measured by Hall effect of different films fabricated by varied precursor ratios from 0.3 to 1.7. Here, precursor ratio is defined as the molar ratio of PbI_2/MAI in the precursor mixture solution. The perovskite films fabricated from precursor ratio of 1.0 were shown to be heavily n-doped with a high electron concentration of $2.8 \times 10^{17}\,cm^{-3}$. It is noted that most of the reported mesoporous perovskite solar cells were fabricated with precursor ratio of 1.0,[18,19] therefore those perovskite films should be n-type. The electronic properties of perovskite films were sensitive to the pre-mixed precursor ratio variation. Reducing the precursor ratio to 0.65 reduced the

electron concentration to $8.1 \times 10^{16}\,cm^{-3}$, while increasing precursor ratio to 1.7 increased the electron concentration to $3.5 \times 10^{18}\,cm^{-3}$. Notably, reducing the precursor ratio to 0.3 converted the perovskite films from n-type to p-type with a hole concentration of $4.0 \times 10^{16}\,cm^{-3}$. This experimental demonstration that the methylammonium lead triiodide can be either n-doped or p-doped by changing the composition verified the unintentional doping prediction of Hong[12] and Yin et al.[13] We want to point out that the composition of the perovskite films should be much different from that in the precursor solution, because the two precursors have different affinities of PEDOT:PSS.[15] Since PbI_2 has a better affinity to PEDOT:PSS than MAI, more MAI than PbI_2 is needed in the precursor mixture solution to form a stoichiometry perovskite film. This explains the n to p-type transition occurred at a much smaller precursor ratio of 0.6 than 1.0 in the precursor solution.

The carrier mobility showed an opposite variation trend with carrier concentration: with increasing precursor ratio, the mobility reduced several times, i.e., from $8.4\,cm^2$/V s for hole mobility in the perovskite films with precursor ratio of 0.3, to 5.4, 3.9, and $1.9\,cm^2$/V s for electron mobility in the perovskite films with precursor ratios of 0.65, 1.0, and 1.7, respectively. The measured carrier mobility for perovskite films made by stoichiometry precursor ratio is close to that reported elsewhere.[20] The reduced carrier mobility with the increased precursor ratio can be explained by the increasing dopant concentration in perovskite films, because the dopants always serve as charge carrier scattering centers.

It is worth pointing out that the doping effect was less likely affected by the impurity phases that may exist in the annealed perovskite films. To clarify this, we have carefully examined the XRD patterns of the perovskite films fabricated by both single- step and two-step methods from different precursor compositions in our previous studies which showed no impurity phase in all the perovskite films, except those made by the single step method with a precursor ratio of 0.35.[15–17] However, the impurity phases in these films are less likely to cause a doping effect because of their much larger bandgap than that of $MAPbI_3$ (1.55 eV). A large optical bandgap of 2.76 eV was derived from the absorption spectra for the impurity phase.

Based on the above analysis, perovskite films can be converted between p-type and n-type by tuning the ratio of the two precursors. To verify it, we designed another experiment to change the composition of a same perovskite film by thermal annealing and observed the conduction type transition. Here, we started from a p-type film formed by the two-step film fabrication process, in which the optimized perovskite films contain excess MAI to fully react with PbI_2.[17] The Hall mobility of the films formed by interdiffusion was $12.8\,cm^2$/V s, higher than that formed by single-step method, which can be explained by the much lower hole concentration in the order of $10^{14}\,cm^{-3}$ in the interdiffusion formed films. Starting with this p-type perovskite film, we reduced the MAI content in this film by thermal annealing. It has been shown by us and several other groups that $MAPbI_3$ is not thermally stable at temperature above 150 °C, which can be explained by the low dissociation energy of $MAPbI_3$.[17,21,22] As expected, Hall effect measurements showed the annealed film turned to n-
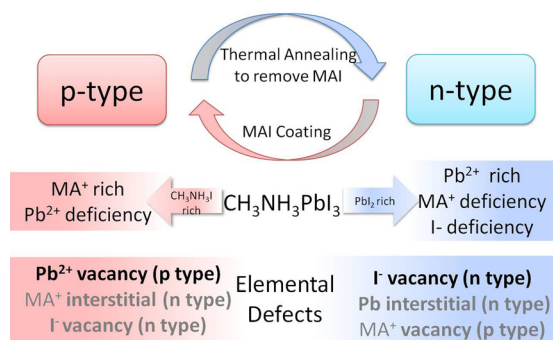
FIG. 2. Schematic conductivity type conversions in perovskite films by excess CH_3NH_3I (left side) or excess PbI_2 (right side). Possible point defects in perovskite films caused by composition variation were illustrated correspondingly. The elemental defects in gray color are less-likely to form in the films, as discussed in the manuscript.

type with an extremely high electron concentration of $7.6 \times 10^{20} \, cm^{-3}$, which is more than six orders of magnitude higher than the hole concentration in the pristine film. Mobility of the high-temperature annealed perovskite film was dramatically reduced to $0.07 \, cm^2/V \, s$, which should be ascribed to the large density of defects caused by the decomposition of the perovskite film. Spin-coating another layer of MAI onto this thermally annealed perovskite film again converted the *n*-type film back to *p*-type. The *n*-, *p*-type conversion by thermal annealing and applying excess MAI is schematically illustrated in Figure 2.

We have shown that PbI_2-rich films are *n*-doped and PbI_2-deficient films are *p*-doped, which is consistent with Yin's calculation results.[13] To understand the origin of self-doping, all the possible composition variation-induced defects in perovskite films are summarized in Figure 2. Left side of the figure listed possible point defects in films with a deficiency of PbI_2, which represents the situation when the precursor ratio is 0.3. Since MAI ratio is much larger than PbI_2, the formed perovskite may possess a lot of Pb and I vacancies due to the deficiency of PbI_2. Calculation result of Yin *et al.* revealed Pb vacancy has much lower formation energy than I

vacancy.[13] We therefore inferred Pb vacancies played a critical role in contributing the *p*-type conductivity in this film. Similar analysis could also be applied to the films with precursor ratio larger than 0.65. Three kinds of point defects may exist in the PbI_2-rich/MAI-deficiency films: Pb interstitial, MA vacancy, and I vacancy. As both Pb interstitials and MA vacancies have too large formation energy based on the calculation results of Yin *et al.*,[13] it is most likely I vacancy causes the *n*-doping behavior in PbI_2 rich films.

We continued to use X-ray photoemission spectroscopy/ ultraviolet photoelectron spectroscopy (XPS/UPS) measurements to verify the composition and process dependent doping type transition between *p* and *n*, and also to investigate its origin. Details about XPS/UPS measurement could be found elsewhere.[23,24] The *p*- to *n*-doping type transition of perovskite should cause the shift of Fermi level across the middle bandgap, which was verified by the UPS results. The energy diagram was constructed by setting the bandgap of all $CH_3NH_3PbI_3$ perovskite films to 1.55 eV, because changed precursor ratio did not change the bandgap. Figure 3 shows the UPS spectra and the derived energy diagram of perovskite films made by different precursor ratio before and after annealing. As shown in Figure 3(b), perovskite films with 1.0 precursor ratio have Fermi level 0.13 eV above the middle bandgap, indicating *n*-doped films. The conductivity type is consistent with our Hall effect measurement as well as UPS results of other group.[25] Further increasing the precursor ratio to 1.7 pushed up the Fermi level to only 0.35 eV below conduction band, resulting in a heavily *n*-doped film. On the other hand, reducing the precursor ratio to 0.65 pushed down the Fermi level closer to valance band top. When precursor ratio was further reduced to 0.3, Fermi level moved 0.08 eV below the middle bandgap, and the film changed to weak *p*-type. It is noteworthy that conductivity type conversion measured by UPS is in good agreement with Hall effect measurement results, which verified the composition-dependent conductivity type of perovskite films. Furthermore, a high temperature annealing of 150 °C for 45 min was applied on the perovskite films formed by 0.3 precursor ratio, aiming to
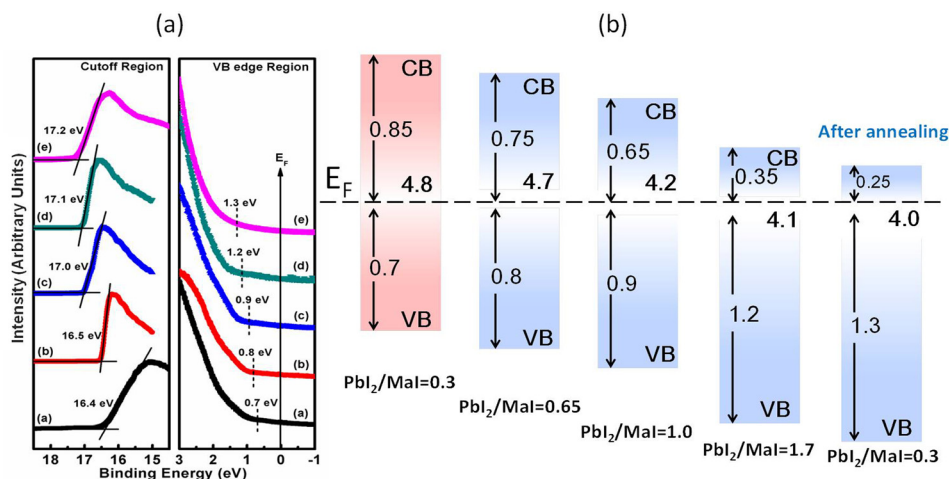

FIG. 3. (a) UPS spectra of the cut-off region and valence band edge region for $CH_3NH_3PbI_3$ films. Spectra a-e represent films deposited by different precursor ratios of 0.3, 0.65, 1.0, 1.7, and 0.3 precursor-ratio film tested after annealing at 150 °C for 45 min, respectively. (b) UPS measured energetic levels of perovskite films formed by one-step method with different precursor ratios of 0.3, 0.65, 1.0, 1.7 (left four columns), and 0.3 precursor-ratio film after annealing at 150 °C for 45 min (right column). E_F, CB, and VB represent Fermi level, conductive band and valence band, respectively. The column colors of pink and blue represent the p- and n-type, respectively.
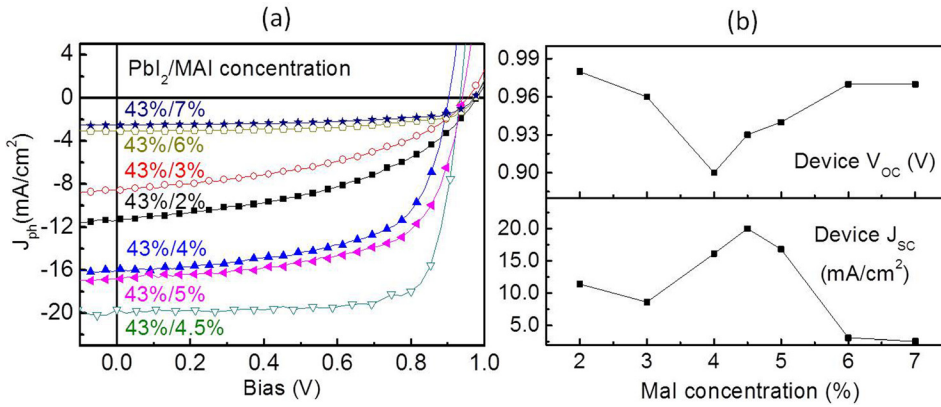
FIG. 4. Photocurrent curves (a) and the corresponding V_{OC}, J_{SC} (b) of the perovskite devices made by interdiffusion method. The perovskite films were made of spun 430 mg/ml PbI_2 films, followed by MAI deposition with varied concentration from 20 mg/ml to 70 mg/ml.

convert these weak *p*-type films into *n*-type by reducing MAI content. The UPS results confirmed the conversion of weak *p*-type sample into heavily doped *n*-type after annealing with Fermi level moving up from below midgap to 0.25 eV below conductive band, which is shown in Figure 3(b). It should be noted that the ionization energy of the perovskite films is sensitive to composition and annealing conditions, and should not be treated as a constant value in energy diagram construction. XPS measurements tracked the composition variation of interdiffusion-made perovskite films before and after conductivity type conversion. Here, we used the composition of Pb as a reference to analyze I variation, because the concentration of Pb in the film is less likely influenced by thermal annealing. The atomic ratio of I to Pb in perovskite film was 3.07: 1 before annealing, which agrees with the scenario of Pb vacancies induced *p*-doping. After annealing for 5 min, the I/Pb atomic ratio reduced to 2.97:1, due to evaporation of CH_3NH_3I from the perovskite film. The reduction of I content in the annealed perovskite film should generate more I vacancies, which is consistent with our claim that I vacancies caused *n*-doping.

Finally, the influence of the doping level on device performance was studied. The changed doping profile should have strong impact on device performance, especially, V_{OC} as it is directly related to quasi-Fermi energy splitting. The relationship of doping level and device V_{OC} can be described by[26]

$$V_{oc} = \frac{kT}{q} \ln\left(\frac{J_{SC}}{J_0} + 1\right), \qquad (3)$$

$$J_0 = \left[\left(\frac{qD_h}{L_h N_d}\right) + \left(\frac{qD_e}{L_e N_a}\right)\right] n_i^2, \qquad (4)$$

where k is Boltzmann constant, T is temperature, q is electron charge, J_{SC} is short circuit current, J_0 is dark saturation current, D_h and D_e are diffusivity of hole and electron, L_h and L_e are diffusion length of holes and electrons, N_d and N_a are concentration of donor and acceptor which determine carrier concentration, and n_i is intrinsic carrier concentration. It is clear for these equations that a larger doping level is needed for larger V_{OC}. However, a too large doping concentration could introduce too many scattering centers, which will reduce carrier mobility and increase charge recombination. In silicon PVs, a moderate doping concentration in the

order of 10^{16} cm^{-3} is optimized for maximum device efficiency.[27]

We fabricated perovskite solar cells with different PbI_2/ MAI ratios by changing the MAI concentration (or thickness) in two-step interdiffusion deposition. The structure of the devices was indium tin oxide (ITO)/PEDOT: PSS/perovskite/[6,6]-phenyl-C61-butyric acid methyl ester (PCBM)/ C_{60}/2,9-dimethyl-4,7-diphenyl-1,10-phenanthroline (BCP)/ Al. Details about device fabrication processes could be found elsewhere.[16] For the perovskite deposition, the concentration of PbI_2 was fixed to 430 mg/ml while the MAI concentration was varied from 20 mg/ml to 70 mg/ml. Figure 4(a) is the performance of devices made by different MAI concentrations. With increased MAI concentration, the device power conversion efficiencies (PCE) first increased and then reduced. The highest average PCE was 14.5% for the device fabricated by 43% PbI_2 and 4.5% MAI solution.

Figure 4(b) summarized the V_{OC} and J_{SC} change in these devices. High V_{OC} was obtained in devices with MAI rich (6%–7%) or MAI deficient (2%–3%) perovskite films. The variation of V_{OC} can be well explained by the doping profiles in these films. Although some parameters, such as J_{SC}, diffusion length, diffusivity, can be changed by varying MAI concentration, doping concentration change should dominate the V_{OC} variation in our perovskite devices, because its change is much more sensitive to composition variation. Perovskite films made by 4.0% MAI solution are weakly *p*-doped with a hole concentration of 4×10^{14} cm^{-3}.[17] Further increasing MAI content in the films by increasing MAI solution concentration to 7% should increase hole concentration, which increased the device V_{OC}. Reducing MAI content converted films from weak *p*-type to moderately doped *n*-type, which explains the larger V_{OC} in these devices. The J_{SC} exhibits an almost opposite variation trend to that of the V_{OC}. The highest J_{SC} was achieved when MAI concentration was 4.5%, whereas increased doping in perovskite films reduced device photocurrents, which can be explained by the doping caused charge recombination.

In conclusion, we demonstrated the electronic properties of perovskite films, i.e., carrier concentration, mobility, conductivity type, and energy level, could be significantly tuned by changing their compositions. The $CH_3NH_3PbI_3$ films formed from the pre-mixed precursor solution with stoichiometry mixed precursors were heavily *n*-doped with an electron concentration of 2.8×10^{17} cm^{-3}. Reducing the

precursor ratio to 0.3 converted the films into weak *p*-type, while increasing the precursor ratio further increased the electron concentration. Thermal annealing was found as another way to convert *p*-type perovskite films into heavily *n*-type through reducing MAI content in the films. Controlling an appropriate doping in perovskite can maximize the device efficiency. This work helps the understanding of the electronic properties of perovskite and may shed light on future rational design of more efficient perovskite solar cells.

[1]K. Walzer, B. Maennig, M. Pfeiffer, and K. Leo, Chem. Rev. **107**, 1233 (2007).

[2]C. Zhang, S. Chen, L. E. Mo, Y. Huang, H. Tian, L. Hu, Z. Huo, S. Dai, F. Kong, and X. Pan, J. Phys. Chem. C **115**, 16418 (2011).

[3]S. D. Stranks, G. E. Eperon, G. Grancini, C. Menelaou, M. J. Alcocer, T. Leijtens, L. M. Herz, A. Petrozza, and H. J. Snaith, Science **342**, 341 (2013).

[4]F. Zhu, P. Zhang, X. Wu, L. Fu, J. Zhang, and D. Xu, ChemPhysChem **13**, 3731 (2012).

[5]Y. Shi, K. K. Kim, A. Reina, M. Hofmann, L.-J. Li, and J. Kong, ACS Nano **4**, 2689 (2010).

[6]Y. Gao, H. L. Yip, K. S. Chen, K. M. O'malley, O. Acton, Y. Sun, G. Ting, H. Chen, and A. K. Y. Jen, Adv. Mater. **23**, 1903 (2011).

[7]M. A. Green, A. Ho-Baillie, and H. J. Snaith, Nat. Photonics **8**, 506 (2014).

[8]N. J. Jeon, J. H. Noh, Y. C. Kim, W. S. Yang, S. Ryu, and S. I. Seok, Nat. Mater. **13**, 897 (2014).

[9]J. Burschka, N. Pellet, S.-J. Moon, R. Humphry-Baker, P. Gao, M. K. Nazeeruddin, and M. Grätzel, Nature **499**, 316 (2013).

[10]M. Liu, M. B. Johnston, and H. J. Snaith, Nature **501**, 395 (2013).

[11]D. Liu and T. L. Kelly, Nat. Photonics **8**, 133 (2014).

[12]J. Kim, S.-H. Lee, J. H. Lee, and K.-H. Hong, J. Phys. Chem. Lett. **5**, 1312 (2014).

[13]W.-J. Yin, T. Shi, and Y. Yan, Appl. Phys. Lett. **104**, 063903 (2014).

[14]W. J. Yin, T. Shi, and Y. Yan, Adv. Mater. **26**, 4653 (2014).

[15]Q. Wang, Y. Shao, Q. Dong, Z. Xiao, Y. Yuan, and J. Huang, Energy Environ. Sci. **7**, 2359 (2014).

[16]Z. Xiao, C. Bi, Y. Shao, Q. Dong, Q. Wang, Y. Yuan, C. Wang, Y. Gao, and J. Huang, Energy Environ. Sci. **7**, 2619 (2014).

[17]C. Bi, Y. Shao, Y. Yuan, Z. Xiao, C. Wang, Y. Gao, and J. Huang, J. Mater. Chem. A **2**, 18508 (2014).

[18]J. H. Heo, S. H. Im, J. H. Noh, T. N. Mandal, C.-S. Lim, J. A. Chang, Y. H. Lee, H.-J. Kim, A. Sarkar, and M. K. Nazeeruddin, Nat. Photonics **7**, 486 (2013).

[19]H.-S. Kim, I. Mora-Sero, V. Gonzalez-Pedro, F. Fabregat-Santiago, E. J. Juarez-Perez, N.-G. Park, and J. Bisquert, Nat. Commun. **4**, 2242 (2013).

[20]C. Wehrenfennig, G. E. Eperon, M. B. Johnston, H. J. Snaith, and L. M. Herz, Adv. Mater. **26**, 1584 (2014).

[21]Q. Chen, H. Zhou, Z. Hong, S. Luo, H.-S. Duan, H.-H. Wang, Y. Liu, G. Li, and Y. Yang, J. Am. Chem. Soc. **136**, 622 (2013).

[22]A. Dualeh, N. Tétreault, T. Moehl, P. Gao, M. K. Nazeeruddin, and M. Grätzel, Adv. Funct. Mater. **24**, 3250 (2014).

[23]X. Liu, S. Yi, C. Wang, I. Irfan, and Y. Gao, Org. Electron. **15**, 977 (2014).

[24]X. Liu, S. Yi, C. Wang, C. Wang, and Y. Gao, J. Appl. Phys. **115**, 163708 (2014).

[25]P. Schulz, E. Edri, S. Kirmayer, G. Hodes, D. Cahen, and A. Kahn, Energy Environ. Sci. **7**, 1377 (2014).

[26]S. O. Kassap, *Principles of Electronic Materials and Devices* (McGraw Hill, New York, U.S.A., 2006).

[27]A. Wang, J. Zhao, and M. Green, Appl. Phys. Lett. **57**, 602 (1990).